Coherent X-Rays Excited by a Relativistic Electron Crossing a Periodic Stratified Structure in Bragg Scattering Geometry

S. V. Blazhevich[a], Yu. P. Gladkikh[a], and A. V. Noskov[b]

[a] *National Research University Belgorod State University, Belgorod, Russia*

[b] *Belgorod University of Cooperation, Economics, and Law, Belgorod, Russia*

Received July 17, 2012

Abstract—The dynamic theory of coherent X-rays excited by a relativistic electron crossing an artificial periodic stratified structure in Bragg scattering geometry has been developed for the general case of asymmetric reflection. Expressions describing the spectral-angular characteristics of radiation have been derived and investigated.

INTRODUCTION

The radiation of a relativistic electron moving through a periodic stratified structure is usually only studied in the Bragg scattering geometry and when reflective amorphous layers of a material are parallel to the input surface of a target, i.e., under the symmetric reflection condition. In [1, 2], radiation observed in a periodic stratified structure was traditionally regarded as resonant-transition radiation. In [3], radiation from a periodic multilayer structure was already regarded as a process whereby pseudophotons of the Coulomb field of a relativistic electron were scattered by the layers of a periodic stratified structure (by analogy with coherent radiation induced by a relativistic electron in crystalline media [4–7]) and represented as the sum of diffracted transition radiation (DTR) and parametric X-ray radiation (PXR). In [3], the radiation process was described via the dynamic approach. In the aforementioned publications, radiation of a relativistic particle penetrating a multilayer medium was investigated only in the Bragg scattering geometry when a particle field is symmetrically reflected by the target surface.

In [8–10], researchers constructed a dynamic theory of the coherent X-rays of a relativistic electron crossing a periodic stratified medium in the Laue scattering geometry when the particle field is asymmetrically reflected by the target surface. As was revealed, the radiation yield corresponding to an artificial periodic structure substantially exceeds that observed in the crystal under analogous conditions. Moreover, it was demonstrated that the photon yield of radiation can also be increased by varying the reflection asymmetry.

In this study, a dynamic theory of the coherent radiation of a relativistic electron moving through a periodic stratified medium is constructed in the Bragg scattering geometry under asymmetric reflection conditions, when the reflective layers of a target are located at an angle to its surface. Expressions describing the spectral-angular characteristics of radiation excited by a relativistic electron crossing an artificial multilayer periodic structure are derived and investigated in the two-wave approximation of dynamic diffraction theory. The mentioned periodic structure is formed by alternating layers of materials with sharply differing dielectric susceptibilities in the radiation-frequency range under consideration. Analysis of the derived expressions indicates that the dynamic diffraction effects detected and investigated for a single-crystal target can appreciably manifest themselves in the radiation of a relativistic electron moving through a periodic stratified structure.

RADIATION-FIELD AMPLITUDE

Let a relativistic electron with velocity $\mathbf{V}$ move through a periodic stratified structure of thickness L in the Bragg scattering geometry (Fig. 1). This structure is formed by periodically positioned amorphous layers with thicknesses of a and b ($T = a + b$ is the structure period) and dielectric susceptibilities of χ_a and χ_b, respectively. In the radiation geometry depicted in Fig. 1, $\boldsymbol{\mu} = \mathbf{k} - \omega\mathbf{V}/V^2$ is the momentum component of a virtual photon perpendicular to the particle velocity $\mathbf{V}$ ($\mu = \omega\theta/V$, where $\theta \ll 1$ is the angle between the vectors $\mathbf{k}$ and $\mathbf{V}$), θ_B is the Bragg angle, and the azimuthal angle φ of radiation is measured from the plane formed by the electron velocity vector $\mathbf{V}$ and the vector $\mathbf{g}$ perpendicular to the reflective layers. The length of vector $\mathbf{g}$ can be represented using the Bragg angle θ_B and Bragg frequency ω_B: $g = 2\omega_B \sin\theta_B/V$.

In [8, 9], dynamic theory of the coherent X-rays of a relativistic electron penetrating a periodic stratified structure was constructed under asymmetric-reflection conditions in the Laue scattering geometry. In the case of asymmetric reflection, the radiation of a relativistic electron crossing a single-crystal target was also examined in the Bragg scattering geometry [11]. When a photon is emitted in the direction $\mathbf{k_g}$, it is possible to perform analytical procedures similar to those described in [8, 9, 11]. Then, the radiation-field amplitude $E_{\mathrm{Rad}}^{(s)}$ can be written as the sum of the contributions from PXR and DTR:

$$E_{\mathrm{Rad}}^{(s)} = E_{\mathrm{PXR}}^{(s)} + E_{\mathrm{DTR}}^{(s)}, \tag{1a}$$

$$\begin{aligned} E_{\mathrm{PXR}}^{(s)} &= \frac{8\pi^2 ieV\theta P^{(s)}}{\omega} \\ &\times \frac{\omega^2\chi_{\mathbf{g}}C^{(s,\tau)}}{2\omega\left(\lambda_{\mathbf{g}}^{(2)}\exp\left(i\frac{\lambda_{\mathbf{g}}^{*}-\lambda_{\mathbf{g}}^{(2)}}{\gamma_{\mathbf{g}}}L\right)-\lambda_{\mathbf{g}}^{(1)}\exp\left(i\frac{\lambda_{\mathbf{g}}^{*}-\lambda_{\mathbf{g}}^{(1)}}{\gamma_{\mathbf{g}}}L\right)\right)} \\ &\times\left[\left(\frac{2\omega\exp\left(i\frac{\lambda_{\mathbf{g}}^{*}-\lambda_{\mathbf{g}}^{(1)}}{\gamma_{\mathbf{g}}}L\right)}{4\frac{\gamma_0^2}{\gamma_{\mathbf{g}}^2}\left(\lambda_{\mathbf{g}}^{*}-\lambda_{\mathbf{g}}^{(2)}\right)}+\frac{\omega}{2\frac{\gamma_0}{|\gamma_{\mathbf{g}}|}\lambda_0^{*}}\right)\right. \\ &\times\left(1-\exp\left(i\frac{\lambda_{\mathbf{g}}^{*}-\lambda_{\mathbf{g}}^{(2)}}{\gamma_{\mathbf{g}}}L\right)\right) \\ &-\left(\frac{2\omega\exp\left(i\frac{\lambda_{\mathbf{g}}^{*}-\lambda_{\mathbf{g}}^{(2)}}{\gamma_{\mathbf{g}}}L\right)}{4\frac{\gamma_0^2}{\gamma_{\mathbf{g}}^2}\left(\lambda_{\mathbf{g}}^{*}-\lambda_{\mathbf{g}}^{(1)}\right)}+\frac{\omega}{2\frac{\gamma_0}{|\gamma_{\mathbf{g}}|}\lambda_0^{*}}\right) \\ &\left.\times\left(1-\exp\left(i\frac{\lambda_{\mathbf{g}}^{*}-\lambda_{\mathbf{g}}^{(1)}}{\gamma_{\mathbf{g}}}L\right)\right)\right], \end{aligned} \tag{1b}$$

$$\begin{aligned} E_{\mathrm{DTR}}^{(s)} &= \frac{8\pi^2 ieV\theta P^{(s)}}{\omega} \\ &\times \frac{\omega^2\chi_{\mathbf{g}}C^{(s,\tau)}}{2\omega\left(\lambda_{\mathbf{g}}^{(2)}\exp\left(-i\frac{\lambda_{\mathbf{g}}^{(2)}}{\gamma_{\mathbf{g}}}L\right)-\lambda_{\mathbf{g}}^{(1)}\exp\left(-i\frac{\lambda_{\mathbf{g}}^{(1)}}{\gamma_{\mathbf{g}}}L\right)\right)} \\ &\times\left[\frac{1}{\frac{\gamma_0}{|\gamma_{\mathbf{g}}|}\left(-\chi_0-\frac{2\gamma_0}{\omega\gamma_{\mathbf{g}}}\lambda_{\mathbf{g}}^{*}+\beta\frac{\gamma_0}{\gamma_{\mathbf{g}}}\right)}+\frac{\omega}{2\frac{\gamma_0}{|\gamma_{\mathbf{g}}|}\lambda_0^{*}}\right] \\ &\times\left(\exp\left(-i\frac{\lambda_{\mathbf{g}}^{(2)}}{\gamma_{\mathbf{g}}}L\right)-\exp\left(-i\frac{\lambda_{\mathbf{g}}^{(1)}}{\gamma_{\mathbf{g}}}L\right)\right). \end{aligned} \tag{1c}$$

Expression (1b) is the amplitude of the PXR field arisen when pseudophotons of the Coulomb field of a

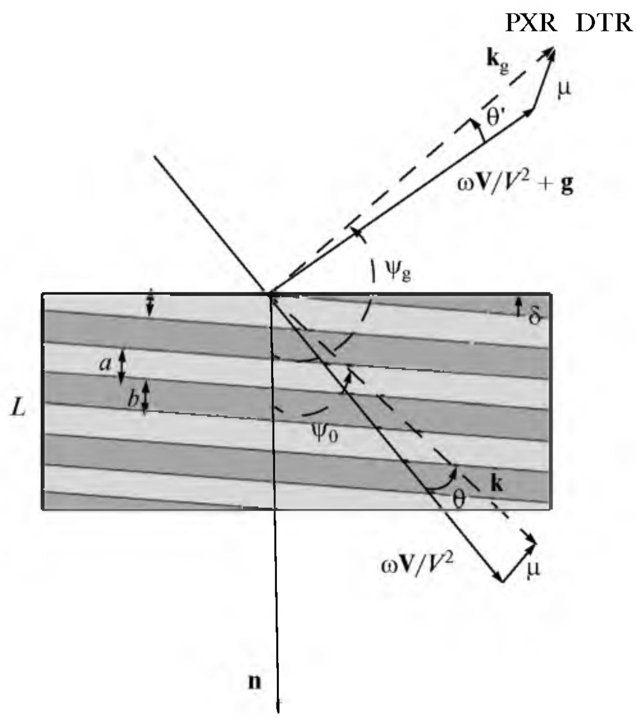

Fig. 1. Geometry of the radiation process, where θ and θ' are the radiation angles; θ_B is the Bragg angle (the angle between the electron velocity $\mathbf{V}$ and the reflective layers); δ is the angle between the surface and layers of a target; and $\mathbf{k}$ and $\mathbf{k_g}$ are the wave vectors of incident and diffracted photons, respectively.

relativistic electron are scattered by the layers of the periodic stratified structure under consideration. Expression (1c) describes the amplitude of the DTR field caused by the fact that transition radiation induced at the input surface is diffracted from the structural layers. According to expression (1b), there are two branches of the solution to the dispersion relationship, which contribute to the PXR yield and correspond to two X-ray waves exited simultaneously with the equilibrium electromagnetic field of a fast particle. The PXR branch, the real part of the denominator of which in (1) can become zero (i.e., $\mathrm{Re}\left(\lambda_{\mathbf{g}}^{*}-\lambda_{\mathbf{g}}^{(1,2)}\right)=0$), makes a larger contribution to radiation. The amplitudes (1) describe σ-polarized fields at $s = 1$ and $\tau = 2$ and π-polarized fields at $s = 2$. Moreover, $\tau = 2$ if $2\theta_B < \frac{\pi}{2}$ and $\tau = 1$ otherwise.

The formulas (1) are based on the following designations:

$$C^{(s,\tau)} = (-1)^{\tau}C^{(s)},\quad C^{(1)} = 1,\quad C^{(2)} = \left|\cos 2\theta_B\right|,$$
$$P^{(1)} = \sin\varphi,\quad P^{(2)} = \cos\varphi;$$

$$\lambda_{\mathbf{g}}^{(1,2)} = \frac{\omega\left|\chi'_{\mathbf{g}}C^{(s)}\right|}{2}\left(\xi^{(s)} - \frac{i\rho^{(s)}(1+\varepsilon)}{2} \pm \sqrt{\xi^{(s)2} - \varepsilon - i\rho^{(s)}((1+\varepsilon)\xi^{(s)} - 2\kappa^{(s)}\varepsilon) - \rho^{(s)2}\left(\frac{(1+\varepsilon)^2}{4} - \kappa^{(s)2}\varepsilon\right)}\right);$$

$$\lambda_{\mathbf{g}}^{*} = \frac{\omega\left|\chi'_{\mathbf{g}}C^{(s)}\right|}{2}\left(2\xi^{(s)} - i\rho^{(s)} - \varepsilon\sigma^{(s)}\right);$$

$$\chi_0(\omega) = \frac{a}{T}\chi_a + \frac{b}{T}\chi_b; \tag{2}$$

$$\chi_{\mathbf{g}}(\omega) = \frac{\exp(-iga) - 1}{igT}(\chi_b - \chi_a);$$

$$\gamma_0 = \cos\psi_0, \quad \gamma_{\mathbf{g}} = \cos\psi_{\mathbf{g}}$$

(where ψ_0 is the angle between the wave vector $\mathbf{k}$ of an incident wave and vector $\mathbf{n}$ normal to the plate surface and $\psi_{\mathbf{g}}$ is the angle between the wave vector $\mathbf{k}_{\mathbf{g}}$ and vector $\mathbf{n}$ (Fig. 1)),

$$\xi^{(s)}(\omega) = \eta^{(s)}(\omega) + \frac{1-\varepsilon}{2\nu^{(s)}},$$

$$\eta^{(s)}(\omega) = \frac{\sin^2\theta_B}{V^2C^{(s)}}\frac{gT}{\left|\chi'_b - \chi'_a\right|\left|\sin\left(\frac{ga}{2}\right)\right|}\left(1 - \frac{\omega(1-\theta\cos\varphi\cot\theta_B)}{\omega_B}\right);$$

$$\nu^{(s)} = \frac{2C^{(s)}\left|\sin\left(\frac{ga}{2}\right)\right|}{g}\left|\frac{\chi'_b - \chi'_a}{a\chi'_a + b\chi'_b}\right|; \tag{3}$$

$$\rho^{(s)} = \frac{a\chi''_a + b\chi''_b}{\left|\chi'_b - \chi'_a\right|C^{(s)}}\frac{g}{2\left|\sin\left(\frac{ga}{2}\right)\right|};$$

$$\kappa^{(s)} = \frac{2C^{(s)}\left|\sin\left(\frac{ga}{2}\right)\right|}{g}\left|\frac{\chi''_b - \chi''_a}{a\chi''_a + b\chi''_b}\right|; \quad \varepsilon = \frac{\gamma_{\mathbf{g}}}{\gamma_0}.$$

The parameter $\nu^{(s)}$ lying in the range $0 \le \nu^{(s)} \le 1$ determines the degree of field reflection from a periodic stratified structure, which depends on the interference of waves reflected from different planes. The behavior of interference can be constructive ($\nu^{(s)} \approx 1$) or destructive ($\nu^{(s)} \approx 0$). The parameter $\rho^{(s)} = \frac{L_{\text{ext}}^{(s)}}{L_{\text{abs}}}$ characterizes the X-ray absorption by a periodic medium and is specified as the ratio between the extinction length $L_{\text{ext}}^{(s)} = \frac{1}{2C^{(s)}\omega}\frac{gT}{\left|\sin\left(\frac{ga}{2}\right)\right|\left|\chi'_b - \chi'_a\right|}$ and the X-ray-absorption length $L_{\text{abs}} = \frac{T}{\omega\left|a\chi''_a + b\chi''_b\right|}$ in the periodic structure. The parameter $\kappa^{(s)}$ indicates the degree of the manifestation of an anomalously low photoabsorption effect (Borrmann effect) when X-ray photons propagate through an artificial periodic multilayer structure. For both crystalline and periodic stratified structures, the necessary condition for observation of the Borrmann effect is $\kappa^{(s)} \approx 1$.

The parameter ε can be represented as $\varepsilon = \sin(\theta_B - \delta)/\sin(\theta_B + \delta)$, where δ is the angle between the input surface of the target and a crystallographic plane. For a fixed value of θ_B, parameter ε specifies the orientation of the input surface of a target with respect to the reflective layers (Fig. 2). With a decrease in the angle $(\theta_B + \delta)$ of electron incidence on the target, parameter δ becomes negative and, thereafter, increases in absolute value (the limiting case is $\delta \to -\theta_B$), thereby enhancing parameter ε. On the contrary, with an increase in incidence angle, the value of ε decreases (in the limiting case, $\delta \to \theta_B$).

SPECTRAL-ANGULAR DENSITY OF RADIATION

Substituting (1) into the known expression [12]

$$\omega\frac{d^2N}{d\omega d\Omega} = \omega^2(2\pi)^{-6}\sum_{s=1}^{2}\left|E_{\text{Rad}}^{(s)}\right|^2, \tag{4}$$

for the spectral-angular density of X-rays, we obtain expressions for the spectral-angular distributions of PXR and DTR and the term describing the interference of mechanisms of these radiations:

$$\omega\frac{d^2N_{\text{PXR}}^{(s)}}{d\omega d\Omega} = \frac{e^2}{\pi^2}\frac{P^{(s)^2}\theta^2}{\left(\theta^2 + \gamma^{-2} - \chi'_0\right)^2}R_{\text{PXR}}^{(s)}, \tag{5a}$$

$$R_{\text{PXR}}^{(s)} = \left|\frac{\Omega_+^{(s)}}{\Delta^{(s)}}\frac{1 - \exp\left(-ib^{(s)}\Delta_+^{(s)}\right)}{\Delta_+^{(s)}} - \frac{\Omega_-^{(s)}}{\Delta^{(s)}}\frac{1 - \exp\left(-ib^{(s)}\Delta_-^{(s)}\right)}{\Delta_-^{(s)}}\right|^2, \tag{5b}$$

$$\omega\frac{d^2N_{\text{DTR}}^{(s)}}{d\omega d\Omega} = \frac{e^2}{\pi^2}P^{(s)^2}\theta^2\left(\frac{1}{\theta^2 + \gamma^{-2} - \chi'_0} - \frac{1}{\theta^2 + \gamma^{-2}}\right)^2 R_{\text{DTR}}^{(s)}, \tag{6a}$$

$$R_{\rm DTR}^{(s)} = \varepsilon^2 \left| \frac{\exp\left(-ib^{(s)}\frac{K^{(s)}}{\varepsilon}\right) - \exp\left(ib^{(s)}\frac{K^{(s)}}{\varepsilon}\right)}{\left(\xi^{(s)} - K^{(s)} - i\rho^{(s)}\frac{1+\varepsilon}{2}\right)\exp\left(-ib^{(s)}\frac{K^{(s)}}{\varepsilon}\right) - \left(\xi^{(s)} + K^{(s)} - i\rho^{(s)}\frac{1+\varepsilon}{2}\right)\exp\left(ib^{(s)}\frac{K^{(s)}}{\varepsilon}\right)} \right|^2, \tag{6b}$$

$$\omega\frac{d^2N_{\rm Int}^{(s)}}{d\omega d\Omega} = \frac{e^2}{\pi^2}P^{(s)^2} \times \frac{\theta^2}{\theta^2 + \gamma^{-2} - \chi_0'}\left(\frac{1}{\theta^2 + \gamma^{-2} - \chi_0'} - \frac{1}{\theta^2 + \gamma^{-2}}\right)R_{\rm Int}^{(s)}, \tag{7a}$$

$$R_{\rm Int}^{(s)} = 2\varepsilon\,{\rm Re}\left(\left(\frac{\Omega_+^{(s)}}{\Delta^{(s)}}\frac{1 - \exp\left(-ib^{(s)}\Delta_+^{(s)}\right)}{\Delta_+^{(s)}} - \frac{\Omega_-^{(s)}}{\Delta^{(s)}}\frac{1 - \exp\left(-ib^{(s)}\Delta_-^{(s)}\right)}{\Delta_-^{(s)}}\right) \times \left(\frac{\exp\left(-ib^{(s)}\frac{K^{(s)}}{\varepsilon}\right) - \exp\left(ib^{(s)}\frac{K^{(s)}}{\varepsilon}\right)}{\left(\xi^{(s)} - K^{(s)} - i\rho^{(s)}\frac{1+\varepsilon}{2}\right)\exp\left(-ib^{(s)}\frac{K^{(s)}}{\varepsilon}\right) - \left(\xi^{(s)} + K^{(s)} - i\rho^{(s)}\frac{1+\varepsilon}{2}\right)\exp\left(ib^{(s)}\frac{K^{(s)}}{\varepsilon}\right)}\right)^*\right), \tag{7b}$$

where the asterisk designates complex conjugation.

The above formulas are written using the following designations:

$$\Delta^{(s)} = \left(\xi^{(s)} - K^{(s)} - i\rho^{(s)}\frac{1+\varepsilon}{2}\right)\exp\left(-ib^{(s)}\Delta_+^{(s)}\right) - \left(\xi^{(s)} + K^{(s)} - i\rho^{(s)}\frac{1+\varepsilon}{2}\right)\exp\left(-ib^{(s)}\Delta_-^{(s)}\right);$$

$$\Omega_\pm^{(s)} = \varepsilon\left(\left(\sigma^{(s)} - i\rho^{(s)}\right)\exp\left(-ib^{(s)}\Delta_\mp^{(s)}\right) + \Delta_\mp^{(s)}\right);$$

$$\Delta_\pm^{(s)} = \frac{\xi^{(s)} \pm K^{(s)}}{\varepsilon} - \sigma^{(s)} + i\frac{\rho^{(s)}(\varepsilon - 1)}{2\varepsilon};$$

$$K^{(s)} = \sqrt{\xi^{(s)2} - \varepsilon - i\rho^{(s)}((1+\varepsilon)\xi^{(s)} - 2\kappa^{(s)}\varepsilon) - \rho^{(s)2}\left(\frac{(1+\varepsilon)^2}{4} - \kappa^{(s)2}\varepsilon\right)};$$
$$b^{(s)} = \frac{1}{2\sin(\theta_{\rm B} + \delta)}\frac{L}{L_{\rm ext}^{(s)}}. \tag{8}$$

Parameter $b^{(s)}$ is the ratio between half of the electron path $L_e = \dfrac{L}{\sin(\theta_{\rm B} + \delta)}$ in the plate and the X-ray extinction length $L_{\rm ext}^{(s)}$ in the periodic stratified medium. Functions $R_{\rm PXR}^{(s)}$ and $R_{\rm DTR}^{(s)}$ describe the PXR and DTR spectra.

THIN NONABSORBING TARGET

Let us consider a target whose thickness is selected so that the electron path L_e in the plate exceeds the X-ray extinction length $L_{\rm ext}^{(s)}$ in the stratified medium. In this case, the condition $b^{(s)} \gg 1$, which indicates the manifestation of dynamic-diffraction effects in the coherent radiation of relativistic electrons moving through a periodic stratified medium, holds true. On the other hand, the target is assumed to be thin enough to disregard the photon-absorption effect in the strat-

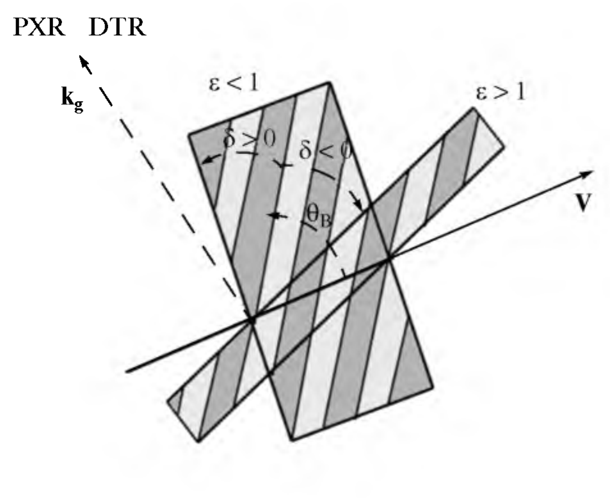

Fig. 2. (ε > 1, ε < 1) Asymmetric reflections of radiation from the target.

ified structure. With this aim in mind, an additional condition is imposed on the target thickness, according to which the maximum path of a diffracted photon crossing the target, $L_{\max f} = \dfrac{L}{\sin(\theta_B - \delta)}$, must be much less than the X-ray absorption length $L_{abs} = \dfrac{T}{\omega\left|a\chi''_a + b\chi''_b\right|}$ in the periodic stratified medium:

$$2\frac{b^{(s)}\rho^{(s)}}{\varepsilon} = \frac{L_{\max f}}{L_{abs}} \ll 1. \tag{9}$$

Let us consider σ-polarized waves ($s = 1$). Using condition (9) with $\rho^{(s)} = 0$ and (5), we obtain the following expression describing the spectral-angular density of PXR in the periodic stratified structure of a thin target:

$$\omega\frac{d^2N^{(1)}_{\mathrm{PXR}}}{d\omega d\Omega} = \frac{e^2}{\pi^2}\frac{\theta_\perp^2}{\left(\theta_\perp^2 + \gamma^{-2} + \dfrac{\left|a\chi'_a + b\chi'_b\right|}{T}\right)^2}R_{\mathrm{PXR}}, \tag{10a}$$

$$R_{\mathrm{PXR}} = R^{(1)}_{\mathrm{PXR}} + R^{(2)}_{\mathrm{PXR}} + R^{(\mathrm{Int})}_{\mathrm{PXR}}, \tag{10b}$$

$$R^{(1)}_{\mathrm{PXR}} = \frac{\left(\xi + \sqrt{\xi^2 - \varepsilon}\right)^2}{\xi^2 - \varepsilon + \varepsilon\sin^2\left(\dfrac{b\sqrt{\xi^2 - \varepsilon}}{\varepsilon}\right)}\frac{\sin^2\left(\dfrac{b^{(1)}}{2}\left(\dfrac{\xi + \sqrt{\xi^2 - \varepsilon}}{\varepsilon} - \sigma\right)\right)}{\left(\dfrac{\xi + \sqrt{\xi^2 - \varepsilon}}{\varepsilon} - \sigma\right)^2}, \tag{10c}$$

$$R^{(2)}_{\mathrm{PXR}} = \frac{\left(\xi - \sqrt{\xi^2 - \varepsilon}\right)^2}{\xi^2 - \varepsilon + \varepsilon\sin^2\left(\dfrac{b^{(1)}\sqrt{\xi^2 - \varepsilon}}{\varepsilon}\right)}\frac{\sin^2\left(\dfrac{b^{(1)}}{2}\left(\dfrac{\xi - \sqrt{\xi^2 - \varepsilon}}{\varepsilon} - \sigma\right)\right)}{\left(\dfrac{\xi - \sqrt{\xi^2 - \varepsilon}}{\varepsilon} - \sigma\right)^2}, \tag{10d}$$

$$R^{(\mathrm{Int})}_{\mathrm{PXR}} = \frac{\varepsilon}{\xi^2 - \varepsilon + \varepsilon\sin^2\left(\dfrac{b^{(1)}\sqrt{\xi^2 - \varepsilon}}{\varepsilon}\right)}\frac{\cos\left(b^{(1)}\dfrac{\sqrt{\xi^2 - \varepsilon}}{\varepsilon}\right)\left(\cos\left(b^{(1)}\left(\dfrac{\xi}{\varepsilon} - \sigma\right)\right) - \cos\left(b^{(1)}\dfrac{\sqrt{\xi^2 - \varepsilon}}{\varepsilon}\right)\right)}{\left(\dfrac{\xi}{\varepsilon} - \sigma\right)^2 + \dfrac{\varepsilon - \xi^2}{\varepsilon^2}}. \tag{10e}$$

In formulas (10), the following designations are introduced:

$$\sigma(\theta, \gamma) = \frac{gT}{2\left|\sin\left(\dfrac{ga}{2}\right)\right|\left|\chi'_b - \chi'_a\right|}\left(\theta_\perp^2 + \gamma^{-2} + \frac{\left|a\chi'_a + b\chi'_b\right|}{T}\right),$$

$$\xi(\omega) = \frac{gT\sin^2\theta_B}{\left|\sin\left(\dfrac{ga}{2}\right)\right|\left|\chi'_b - \chi'_a\right|}\left(1 - \frac{\omega}{\omega_B}\right) + \frac{1+\varepsilon}{2\nu^{(1)}},$$

$$b^{(1)} = \frac{2\omega_B\left|\sin\left(\dfrac{ga}{2}\right)\right|\left|\chi'_b - \chi'_a\right|}{gT\sin(\theta_B + \delta)}L, \quad \theta_\perp = \theta\sin\varphi. \tag{11}$$

The spectral density of PXR is represented as the sum of contributions from two X-ray waves excited in the target (functions $R^{(1)}_{\mathrm{PXR}}$ and $R^{(2)}_{\mathrm{PXR}}$) and the term $R^{(\mathrm{Int})}_{\mathrm{PXR}}$ corresponding to their interference.

According to expressions (6) and (7), we obtain formulas for the spectral-angular density of DTR and the term describing the influence of interference between DTR and PXR in the thin nonabsorbing target:

$$\omega\frac{d^2N^{(1)}_{\mathrm{DTR}}}{d\omega d\Omega} = \frac{e^2}{\pi^2}\theta_\perp^2\left(\frac{1}{\theta_\perp^2 + \gamma^{-2}} - \frac{1}{\theta_\perp^2 + \gamma^{-2} + \dfrac{\left|a\chi'_a + b\chi'_b\right|}{T}}\right)^2 R_{\mathrm{DTR}}, \tag{12a}$$

$$R_{\mathrm{DTR}} = \frac{\varepsilon^2}{\xi^2 - (\xi^2 - \varepsilon)\coth^2\left(\frac{b^{(1)}\sqrt{\varepsilon - \xi^2}}{\varepsilon}\right)}, \tag{12b}$$

$$\omega\frac{d^2N_{\mathrm{Int}}^{(s)}}{d\omega d\Omega} = \frac{e^2}{\pi^2}\frac{\theta_\perp^2}{\theta_\perp^2 + \gamma^{-2} + \frac{|a\chi'_a + b\chi'_b|}{T}}\left(\frac{1}{\theta_\perp^2 + \gamma^{-2}} - \frac{1}{\theta_\perp^2 + \gamma^{-2} + \frac{|a\chi'_a + b\chi'_b|}{T}}\right)R_{\mathrm{Int}}, \tag{13a}$$

$$R_{\mathrm{Int}}^{(s)} = \frac{2\varepsilon^3}{\xi^2 - \varepsilon + \varepsilon\sin^2\left(\frac{b^{(1)}\sqrt{\xi^2 - \varepsilon}}{\varepsilon}\right)} \frac{\sigma\sqrt{\xi^2 - \varepsilon}\sin\left(\frac{b^{(1)}\sqrt{\xi^2 - \varepsilon}}{\varepsilon}\right)\sin\left(b^{(1)}\left(\frac{\xi}{\varepsilon} - \sigma\right)\right) + (\sigma\xi - 1)\sin^2\left(\frac{b^{(1)}\sqrt{\xi^2 - \varepsilon}}{\varepsilon}\right)}{(\xi - \varepsilon\sigma)^2 + \varepsilon - \xi^2}. \tag{13b}$$

Expressions (10)–(13) derived above are the main result of this study. They make it possible to investigate the spectral-angular characteristics of the coherent radiation of a relativistic electron crossing a periodic stratified structure in the Bragg scattering geometry with allowance for dynamic-diffraction effects.

ANALYSIS OF THE SPECTRAL-ANGULAR DENSITY OF RADIATION

The first and second branches of the X-ray waves excited in the target, which are defined, respectively, by the functions $R_{\mathrm{PXR}}^{(1)}$ (10c) and $R_{\mathrm{PXR}}^{(2)}$ (10d), noticeably contribute to the PXR spectrum only if equations

$$\frac{\xi(\omega) + \sqrt{\xi(\omega)^2 - \varepsilon}}{\varepsilon} - \sigma = 0, \tag{14a}$$

$$\frac{\xi(\omega) - \sqrt{\xi(\omega)^2 - \varepsilon}}{\varepsilon} - \sigma = 0. \tag{14b}$$

have solutions corresponding to zero denominators in their expressions.

It can be shown that the first branch ($R_{\mathrm{PXR}}^{(1)}$) contributes more significantly to the spectrum than the second branch ($R_{\mathrm{PXR}}^{(2)}$). Indeed, the contributions of $R_{\mathrm{PXR}}^{(1)}$ and $R_{\mathrm{PXR}}^{(2)}$ are comparable only at very small values of the asymmetry parameter, i.e., at $\varepsilon \ll 1$. However, this condition leads to the very small yield of PXR.

Let us consider the spectral density of PXR at different observation angles. Figure 3 presents curves describing the PXR spectrum of a relativistic electron with an energy of $E = 500$ MeV crossing a periodic stratified beryllium–silicon medium, which were calculated from formulas (10a) and (10c) for the parameters indicated in the figure. It is seen that the PXR spectrum is shifted to the frequency region corresponding to the total external reflection (extinction) of radiation with decreasing observation angle $\theta_\perp$. The total external reflection region is defined by the inequality

$$-\sqrt{\varepsilon} < \xi(\omega) < \sqrt{\varepsilon}, \tag{15}$$

where $\xi(\omega) = \frac{gT\sin^2\theta_{\mathrm{B}}}{\left|\sin\left(\frac{ga}{2}\right)\right||\chi'_b - \chi'_a|}\left(1 - \frac{\omega}{\omega_{\mathrm{B}}}\right) + \frac{1+\varepsilon}{2\nu^{(1)}}$.

Let us consider the spectral density of DTR at different observation angles. Figure 4 presents curves describing the DTR spectrum, which were calculated from formulas (12a) and (12b) for parameter values equal to those in Fig. 3. As can be seen in Fig. 4, the amplitude of the DTR spectrum varies with observation angle $\theta_\perp$. However, the total external reflection region (15) remains unchanged because the spectral function $\xi(\omega)$ is independent of the observation angle.

Let us analyze the dependence of the spectral density of radiation on the ratio between the thicknesses b and a of the reflective layers. Figures 5 and 6 depict, respectively, the curves of the spectral densities of PXR and DTR, which were constructed at different b/a ratios under the assumption of a fixed structure period $T = a + b$. It follows from Figs. 5 and 6 that two radiation mechanisms exhibit the maximum spectral density at $b/a \approx 1$. This is explained by the fact that, for the Be–Si structure under consideration, parameter $\nu^{(1)}$ in (3) (its value characterizes the degree of wave reflection from a periodic stratified structure, which is caused by the character of the interference of waves reflected by different medium layers) reaches its maximum if $b/a \approx 1$.

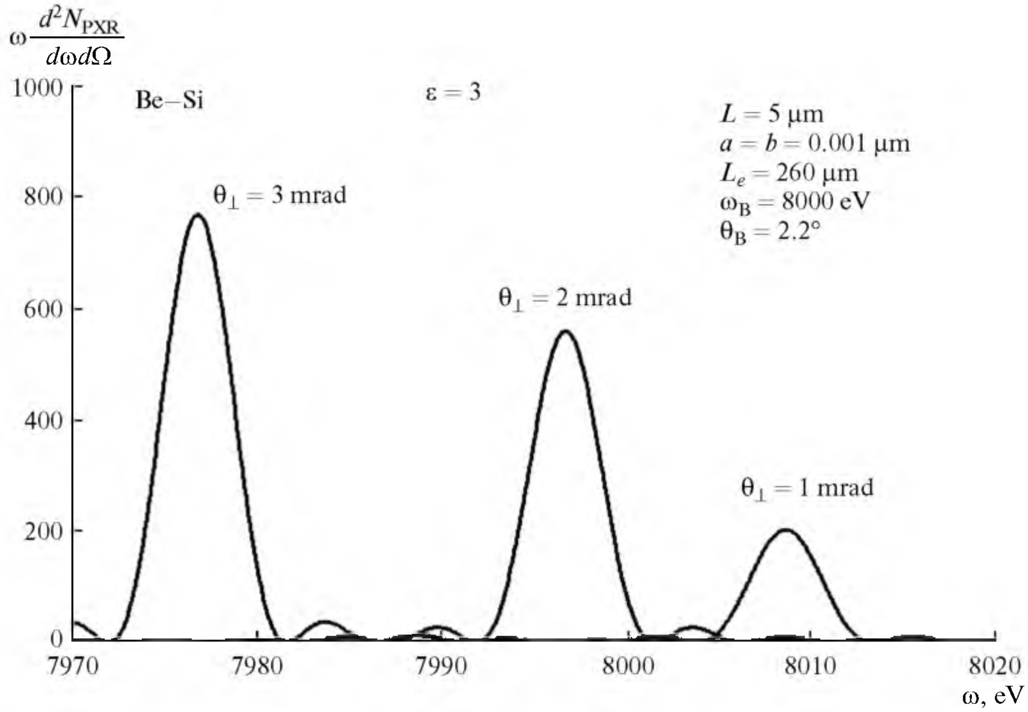

Fig. 3. PXR spectra of a relativistic electron moving through a periodic stratified medium at different observation angles.

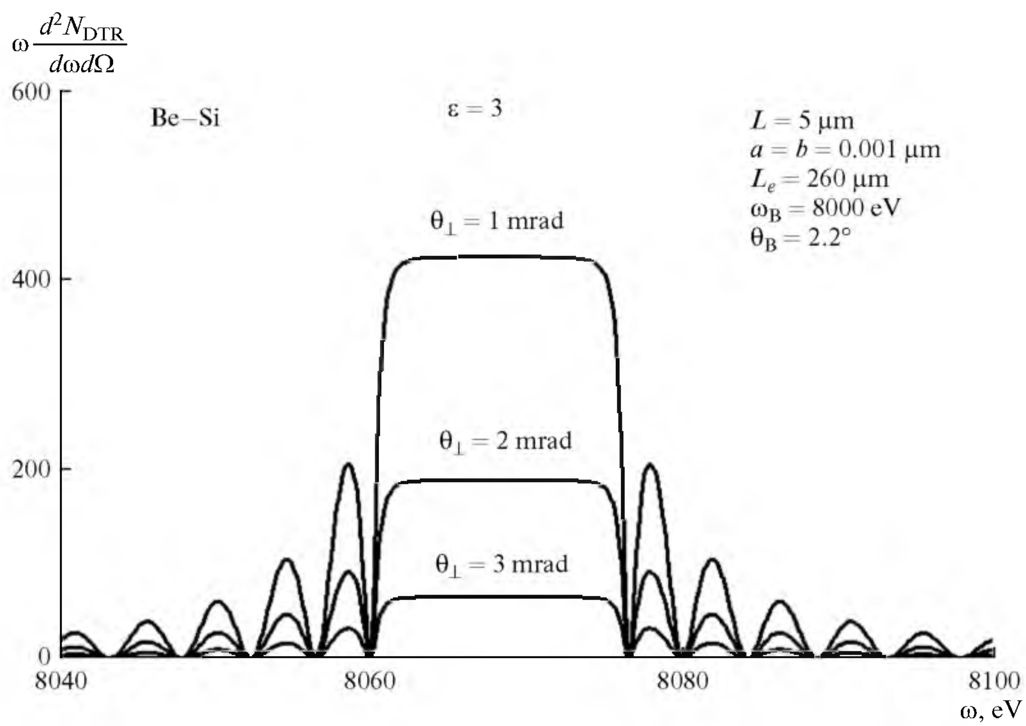

Fig. 4. DTR spectra of a relativistic electron moving through a periodic stratified medium at different observation angles.

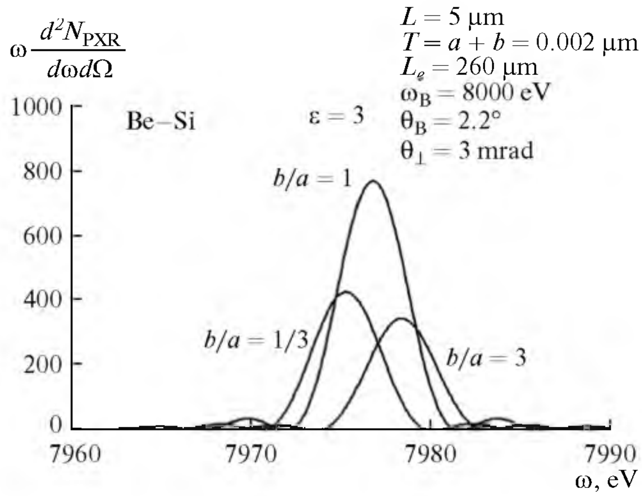

Fig. 5. PXR spectra at different ratios of the layer thicknesses b and a. The structure period $T = a + b$ is fixed.

To analyze the dependence of ν on the b/a ratio, this parameter is represented as

$$\nu = \frac{1}{\pi}\left(1+\frac{b}{a}\right)\left|\frac{\chi'_b}{\chi'_a}-1\right|\frac{\sin\left(\frac{\pi}{1+\frac{b}{a}}\right)}{1+\frac{b}{a}\frac{\chi'_b}{\chi'_a}}. \quad (16)$$

Figure 7 presents the curves calculated from formula (16) for Be–Si and Be–W structures. As is seen in the figure, the degree of reflection of the denser W medium is higher and the shifted maximum of the radiation density is observed. It is necessary to note that the frequency region of total external reflection (Fig. 6) is shifted with a change in the ratio between the thicknesses b and a due to the dependence between the spectral function $\xi(\omega)$ and this ratio.

Let us consider the influence of field-reflection asymmetry with respect to the target surface on the spectral-angular characteristics of PXR and DTR. Figures 8 and 9 depict, respectively, curves describing the spectral densities of PXR and DTR for different values of the asymmetry parameter ε, which were constructed at a fixed electron path L_e = 260 μm. As is seen in Fig. 8, an increase in asymmetry, i.e., a decrease in the angle of electron incidence on the target surface, substantially enhances the spectral width of PXR, if the Bragg angle θ_B is fixed. This is related to fact that the frequency dependence of the resonance condition (14a) becomes weaker with increasing parameter ε. It follows from Fig. 9 that reflection asymmetry also affects the DTR spectrum. In this case, an increase in ε enhances both the spectral amplitude and the frequency region of total external reflection, which also depends on the asymmetry. When the reflection asymmetry is enhanced, an increase in the spectral densities of PXR and DTR leads to an appreciable increase in the angular densi-

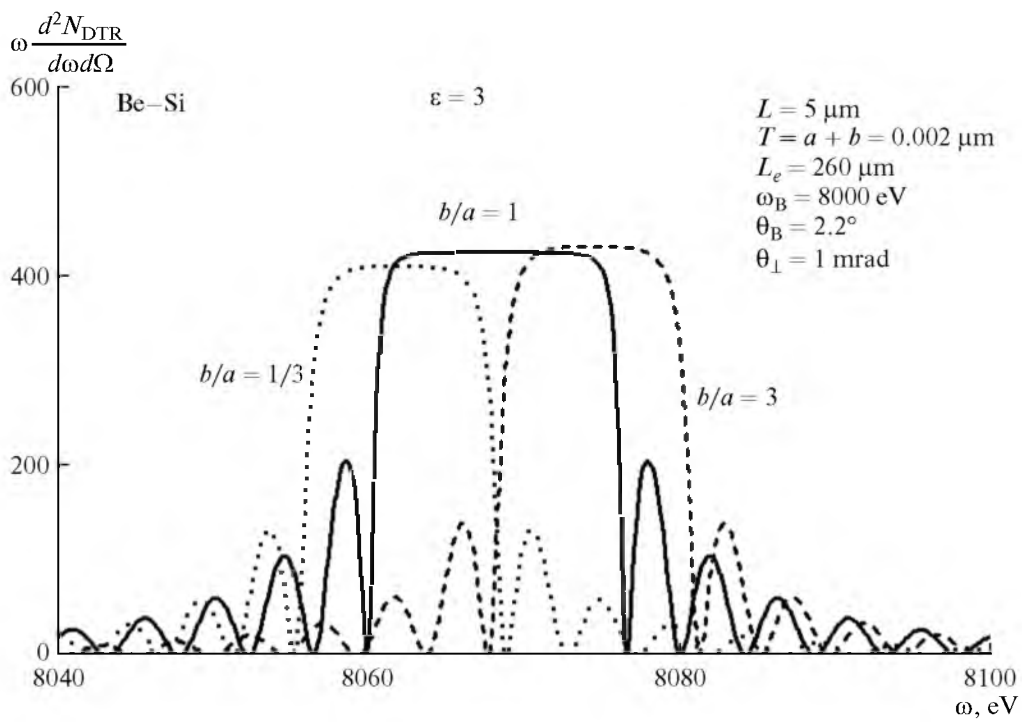

Fig. 6. DTR spectra at different ratios of the layer thicknesses b and a. The structure period $T = a + b$ is fixed.

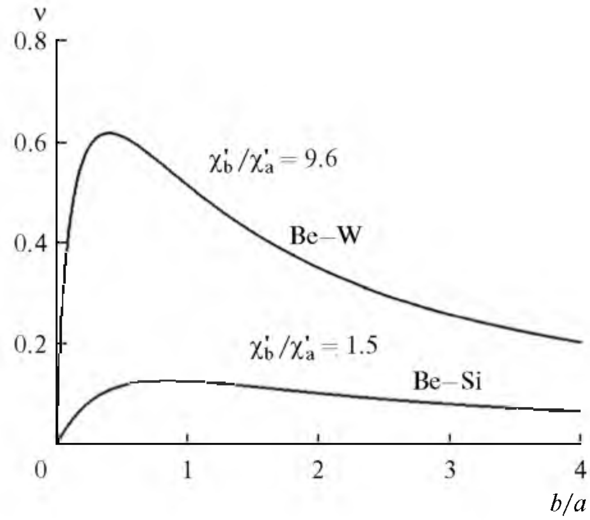

Fig. 7. Dependences between parameter ν used to determine the degree of X-ray reflection from a periodic structure and the b/a ratio for two structures.

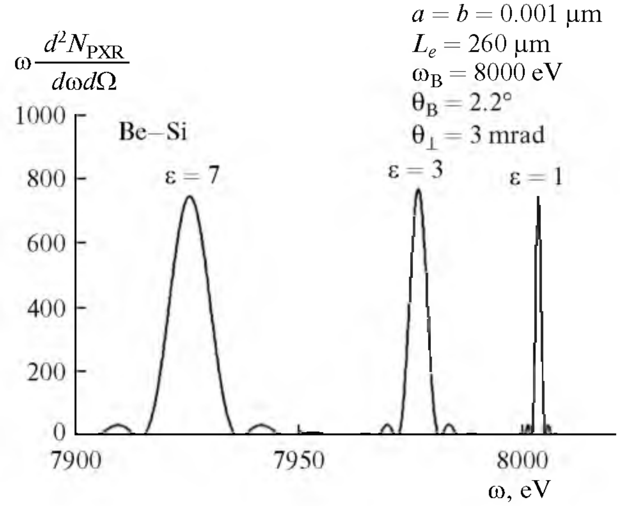

Fig. 8. Influence of reflection asymmetry (parameter ε) on the spectral density of PXR at a fixed observation angle.

ties of radiations. To confirmed the aforesaid, it is possible to utilize the following formulas describing the angular densities of radiation:

$$\frac{dN_{\mathrm{PXR}}}{d\Omega} = \frac{e^2}{\pi^2}\frac{\theta_\perp^2}{\left(\theta_\perp^2+\gamma^{-2}+\frac{\left|a\chi'_a+b\chi'_b\right|}{T}\right)^2}\int_{-\infty}^{+\infty} R_{\mathrm{PXR}}\frac{d\omega}{\omega}, \quad (17)$$

$$\frac{dN_{\mathrm{DTR}}}{d\Omega} = \frac{e^2}{\pi^2}\theta_\perp^2$$
$$\times\left(\frac{1}{\theta_\perp^2+\gamma^{-2}}-\frac{1}{\theta_\perp^2+\gamma^{-2}+\frac{\left|a\chi'_a+b\chi'_b\right|}{T}}\right)^2\int_{-\infty}^{+\infty} R_{\mathrm{DTR}}\frac{d\omega}{\omega}. \quad (18)$$

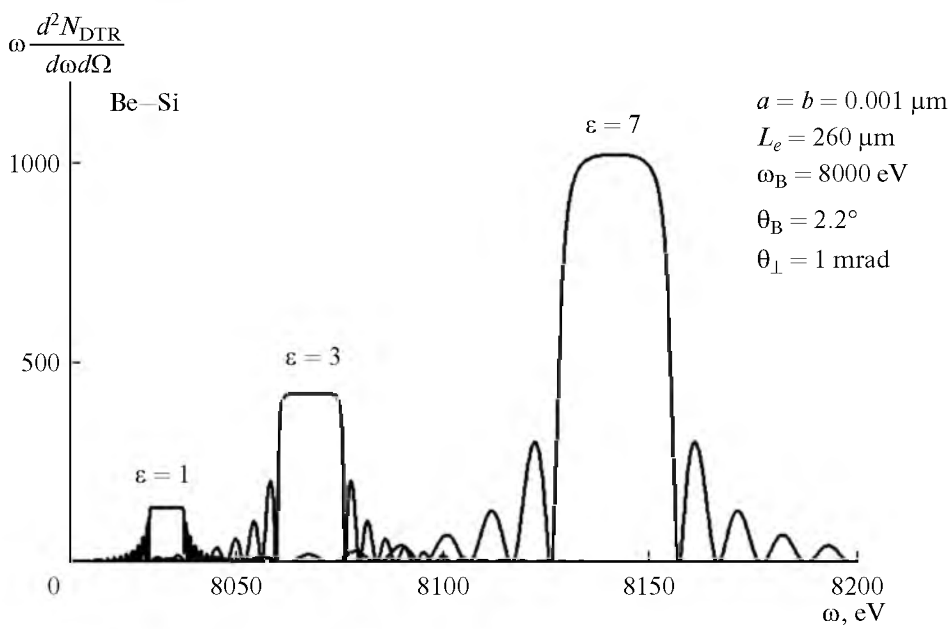

Fig. 9. Influence of reflection asymmetry (parameter ε) on the spectral density of DTR at a fixed observation angle.C

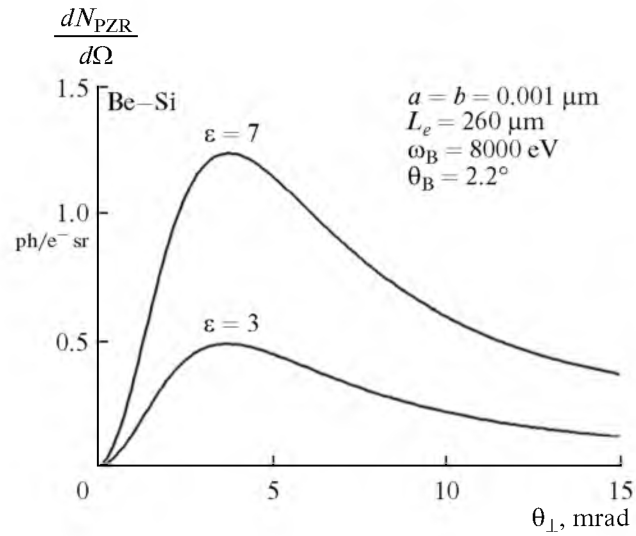

Fig. 10. Variations in the angular density of PXR for different parameters of reflection asymmetry.

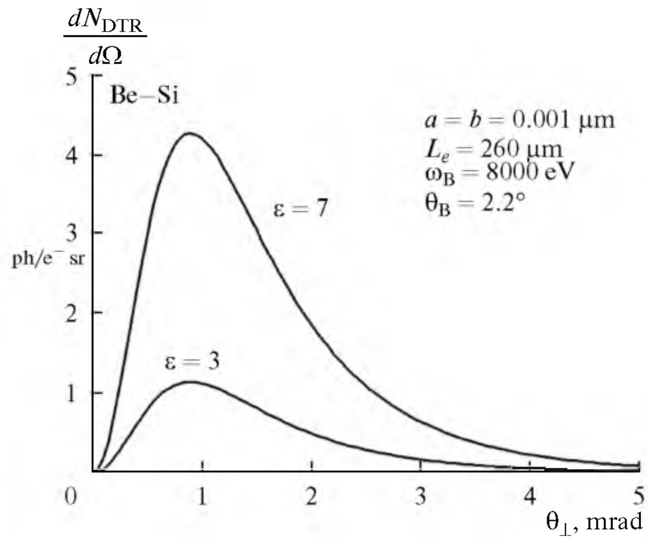

Fig. 11. Variations in the angular density of DTR for different parameters of reflection asymmetry.

Figures 10 and 11 present the angular distributions of radiation calculated according to formulas (17) and (18). As is clear from the constructed curves, an increase in parameter ε noticeably enhances the angular densities of PXR and DTR.

CONCLUSIONS

This study has been carried out to develop the theory of the coherent X-ray waves of a relativistic electron crossing a periodic stratified structure in the Bragg scattering geometry. By analogy with waves a relativistic electron moving through a single-crystal medium, the corresponding coherent X-ray waves induced in the periodic stratified medium are interpreted as the sum of contributions from parametric X-ray radiation and diffracted transition radiation. Expressions describing the spectral-angular characteristics of PXR and DTR of a relativistic electron crossing a periodic stratified structure are derived using the two-wave approximation of dynamic diffraction theory. The spectral-angular densities of radiation are revealed to depend on both the ratio between the thicknesses of the medium layers and the asymmetry of X-ray field scattering by the stratified structure. In particular, it is demonstrated that, at a fixed Bragg angle, a decrease in the angle of electron incidence on the stratified structure (i.e., an increase in the asymmetry parameter ε) substantially increases the PXR-spectrum width, simultaneously leading to an increase in the angular density (the given effect is established to be independent of absorption). A decrease in the angle of electron incidence on the target is ascertained to increase the frequency region of total external reflection and, as a consequence, the spectrum width. As a result, a significant increase in the angular density of DTR is observed.

REFERENCES

1. M. L. Ter-Mikaelyan, *The Influence of the Medium on High-Energy Electromagnetic Processes* (AN ArmSSR, Yerevan, 1969), p. 459 [in Russian].
2. M. A. Piestrup, D. G. Boyers, C. I. Pincus, et al., Phys. Rev. A **45**, 1183 (1992).
3. N. N. Nasonov, V. V. Kaplin, S. R. Uglov, M. A. Piestrup, and C. K. Gary, Phys. Rev. E **68**, 3604 (2003).
4. G. M. Garibyan and Yan Shi, Sov Phys. JETP **34**, 495 (1971).
5. V. G. Baryshevskii and I. D. Feranchuk, Sov. Phys. JETP **34**, 502 (1971).
6. V. G. Baryshevsky and I. D. Feranchuk, J. Phys. (Paris) **44**, 913 (1983).
7. A. Caticha, Phys. Rev. A **40**, 4322 (1989).
8. S. V. Blazhevich, I. V. Kolosova, and A. V. Noskov, J. Exp. Theor. Phys. **114**, 547 (2012).
9. S. V. Blazhevich, I. V. Kolosova, and A. V. Noskov, J. Surf. Invest. **6**, 348 (2012).
10. S. Blazhevich, I. Kolosova, and A. Noskov, J. Phys.: Conf. Ser. **357**, 012016 (2012). doi:10.1088/1742-6596/357/1/012016
11. S. V. Blazhevich and A. V. Noskov, J. Surf. Invest. **5**, 364 (2011).
12. V. A. Bazylev and N. K. Zhevago, *Radiation of Fast Particles in Matter and External Fields* (Nauka, Moscow, 1987) [in Russian].